Discrete and continuous disorder in superlattices

J.-P. Locquet, D. Neerinck, L. Stockman, and Y. Bruynseraede
Laboratorium voor Vaste Stof-Fysika en Magnetisme, Katholieke Universiteit Leuven, B-3030 Leuven, Belgium

Ivan K. Schuller
Physics Department-B019, University of California–San Diego, La Jolla, California 92093
(Received 12 September 1988; revised manuscript received 24 January 1989)

We have derived a general diffraction relation for crystalline-crystalline superlattices including discrete fluctuations on the number of atoms in a layer and continuous fluctuations on the interface distance, both of a Gaussian type. We show that discrete fluctuations can markedly increase the linewidth of high-angle (large-q) diffraction peaks in lattice-mismatched systems. Moreover, we show that this line broadening increases strongly with increasing lattice mismatch and prove that these fluctuations on lattice-matched systems such as semiconductor superlattices are difficult to detect by high-angle diffraction techniques. These results have serious implications for the classical interpretation of x-ray diffraction from superlattices regarding the determination of elastic strains and the reconstruction of composition profiles.

The effect of layering on the structural properties of metallic and semiconductor superlattices has received considerable attention in recent years.[1,2] It was shown that it is possible to achieve superlattice growth of materials with a large lattice mismatch and different crystal symmetry.[3] Several structural models have been developed taking into account various degrees of structural imperfections, which can influence seriously the electrical, magnetic, or mechanical properties of layered structures.

X-ray diffraction (θ-2θ) has been commonly used to verify and characterize the compositional and strain modulation in superlattices.[1,2] The linewidth of the high-angle reflections in metallic superlattices is much larger than predicted by simple one-dimensional models, such as the "step" and the "strain" models.[4,5] The structural coherence length $\xi_\perp$ in metallic superlattices rarely exceeds a few times the modulation wavelength Λ, indicating that a mechanism reducing the long-range order is effective. In recent works,[6–8] we showed that *continuous* fluctuations on the interface distance (i.e., the distance at the interface between the atoms of material A and B) can explain the loss of long-range order. The derived amount of disorder was of the order of the lattice mismatch (i.e., $\cong 0.3$ Å in Nb/Cu, $\Lambda = 30$ Å, lattice mismatch $\cong 0.25$ Å) but is not compatible with the presence of only a few low-angle peaks.

A small amount of disorder as derived from x-ray spectra, may drastically affect the transport properties of multilayers. For instance, in lattice-matched Nb/Ta superlattices[9] with a structure which is claimed to be perfect, the electronic mean free path l is claimed to be much longer than Λ. However, a small amount of interfacial disorder ($\cong 0.3$ Å) as found in Nb/Cu superlattices, is sufficient to severely limit l to the layer thickness. These facts indicate that a small structural disorder has a much more pronounced effect on the electric properties than on the x-ray spectra.

Different mechanisms can cause disorder: (i) imperfections in the deposition process, (ii) geometric constraints at the interfaces due to the differences in lattice parameter and symmetry, (iii) variations in growth mode and wetting, and (iv) interdiffusion and alloying. In practice, all these conditions limit the control over the thickness of the individual layers to approximately a few percent. As a result, the number of atoms in a crystalline layer will fluctuate from layer to layer as well as in the plane of the layer, following roughly a Gaussian distribution of a discrete type. Furthermore, depending on the nucleation process, large deviations from the layer-by-layer growth can occur. On the other hand, the geometric constraints can be accommodated by distorting the layers or the interfaces if the lattice mismatch is sufficiently small so that, energetically, such distortions are allowed.

Structural imperfections can be modeled as Gaussian type of fluctuations, on the modulation wavelength,[10,11] number of atoms in a layer,[12] interface distance,[6,7] layer thickness,[13,14] parallel,[15] and perpendicular to the interfaces. We must distinguish between continuous fluctuations, originating from an amorphous interface, for instance, and discrete fluctuations, resulting from crystalline interfaces. It was shown[13] that the former distribution with width $c^{-1} = 2$ Å, on the thickness of the amorphous layer, explains the total loss of high-angle superlattice peaks in crystalline-amorphous systems. At high-angle (large q), it was reported that the latter distribution of width c^{-1} equal to an atomic distance (in crystalline-amorphous systems) gives rise to a slight reduction in diffraction-peak intensity and a disappearance of the secondary fringes.[12]

In this paper, we derive a kinematical diffraction relation for crystalline-crystalline superlattices including interfacial disorder (induced by the lattice mismatch), as well as disorder due to *discrete* fluctuations in the number of atoms composing a given layer. This relation is first applied to Nb/Cu superlattices, and used to calculate

 ©1989 The American Physical Society

low-angle as well as high-angle diffraction spectra. The Nb/Cu system is expected to form superlattices with sharp interfaces because the constituents do not form any alloys in their thermodynamic phase diagram. Coherency strains were not reported for this system, justifying the use of bulk lattice spacings. In the second part we study the influence of the lattice mismatch on the line broadening induced by discrete fluctuations. These results may have important implications for structural studies of lattice-matched semiconducting (for instance, GaAs/GaAlAs) and metallic (for instance, Nb/Ta) superlattices.

As in our previous work,[6,7] we assume that the distance at the interface between atoms of the different constituents is not constant throughout the multilayer, but fluctuates around an average value $\bar{a}$ following a continuous, Gaussian distribution of width c_0^{-1}. The lattice mismatch can be the origin of this fluctuation. Furthermore, we suppose that the number of atoms in a layer of material A is not constant but fluctuates around an average $\bar{N}$, following a discrete Gaussian distribution, with width c_N^{-1}. For material B we use similar assumptions $(\bar{M}, c_M^{-1})$. Figure 1 gives a pictorial representation of this model.

The structure factor $F(q)$ can be written as

$$
\begin{aligned}
F(q)= & \sum_{n=0}^{N_1-1} f_a \exp(iqnd_a)+f_b \exp\{iq[(N_1-1)d_a+a_1]\} \\
& \times \sum_{m=0}^{M_1-1} \exp(iqmd_b)+\exp\{iq[(N_1-1)d_a+a_1+(M_1-1)d_b+a_2]\} \\
& \qquad \times \left[\sum_{n=0}^{N_2-1} f_a \exp(iqnd_a)+f_b \exp\{iq[(N_2-1)d_a+a_3]\} \sum_{m=0}^{M_2-1} \exp(iqmd_b) \right] + \cdots \\
& + \exp\left[iq \left[\sum_{n=1}^{P-1} [(N_n-1)d_a+a_{2n-1}+(M_n-1)d_b+a_{2n}] \right] \right] \\
& \times \left[\sum_{n=0}^{N_P-1} f_a \exp(iqnd_a)+f_b \exp\{iq[(N_p-1)d_a+a_{2p-1}]\} \sum_{m=0}^{M_p-1} \exp(iqmd_b) \right] ,
\end{aligned} \tag{1}
$$

with N_n, M_n the respective number of atoms in the considered nth plane, and a_n the value of nth interfacial distance. P is the number of crystalline blocks of material A (lattice spacing d_a, scattering power f_a, average number of planes $\bar{N}$) and material B (lattice spacing d_b, scattering power f_b, average number of planes $\bar{M}$).

We calculate $F(q)F^*(q)$ and make the average by integrating over all real interface distances and summing over all integer values. In this relation we use the following symbols for expressions where only the average value of our parameters are involved:

$$
\begin{aligned}
S_N &= \sin(qd_a\bar{N}/2) , \\
C_N &= \cos(qd_a\bar{N}/2) , \\
S_a &= \sin(qd_a/2) , \\
S_M &= \sin(qd_b\bar{M}/2) , \\
C_N &= \cos(qd_b\bar{M}/2) , \\
S_b &= \sin(qd_b/2) , \\
\Lambda &= (\bar{N}-1)d_a+(\bar{M}-1)d_b+2\bar{a} , \\
C_{(2k-1)\Lambda/2} &= \cos[q(2k-1)\Lambda/2] , \\
C_{k\Lambda} &= \cos(qk\Lambda) , \\
S_{(2k-1)\Lambda/2} &= \sin[q(2k-1)\Lambda/2] , \\
S_{k\Lambda} &= \sin(qk\Lambda) .
\end{aligned} \tag{2}
$$

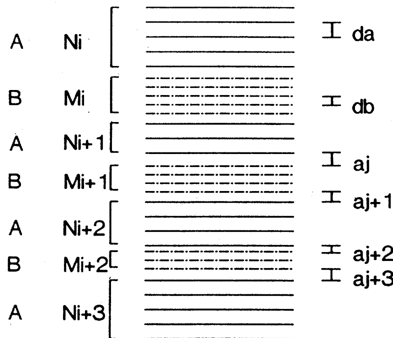

FIG. 1. Model of the superlattice used in the simulations.

Additional symbols are used for functions which are averaged over the discrete distributions:

$$\Phi_a \equiv \langle \sin^2(qd_a k/2) \rangle = \sum_{k=-\infty}^{+\infty} K_a \sin^2(qd_a k/2) \exp(-k^2 c_N^2) ,$$

$$\Phi_b \equiv \langle \sin^2(qd_b k/2) \rangle = \sum_{k=-\infty}^{+\infty} K_b \sin^2(qd_b k/2) \exp(-k^2 c_M^2) ,$$

$$\Delta_a \equiv \langle \cos(qd_a k) \rangle = \sum_{k=-\infty}^{+\infty} K_a \cos(qd_a k) \exp(-k^2 c_N^2) ,$$

$$\Delta_b \equiv \langle \cos(qd_b k) \rangle = \sum_{k=-\infty}^{+\infty} K_b \cos(qd_b k) \exp(-k^2 c_M^2) , \tag{3}$$

with K_a and K_b the normalization constants for the discrete distributions. With these symbols the intensity can be written as

$$\begin{aligned} I(q) = P \left[f_a^2 \frac{S_N^2(1-2\Phi_a)+\Phi_a}{S_a^2} + f_b^2 \frac{S_M^2(1-2\Phi_b)+\Phi_b}{S_b^2} \right] \\ +2\sum_{k=1}^{P} \Bigg\{ [2P-(2k-1)] \Bigg[f_a f_b \frac{\Delta_a^{k-1}\Delta_b^{k-1}}{S_a S_b} \\ \times [S_N S_M C_{(2k-1)\Lambda/2}(1-\Phi_a)(1-\Phi_b) - S_N C_M S_{(2k-1)\Lambda/2}(1-\Phi_a)(\Phi_b) \\ - S_M C_N S_{(2k-1)\Lambda/2}(\Phi_a)(1-\Phi_b) - C_N C_M C_{(2k-1)\Lambda/2}(\Phi_a)(\Phi_b)] \\ \times \exp\left[-\frac{(2k-1)q^2}{4c_0^2} \right] \Bigg] \\ +(P-k) \Bigg[f_a^2 \frac{\Delta_a^{k-1}\Delta_b^{k}}{S_a^2} [S_N^2 C_{k\Lambda}(1-\Phi_a)^2 - 2S_N C_N S_{k\Lambda}(1-\Phi_a)\Phi_a - C_N^2 C_{k\Lambda}\Phi_a^2] \\ + f_b^2 \frac{\Delta_a^{k}\Delta_b^{k-1}}{S_b^2} [S_M^2 C_{k\Lambda}(1-\Phi_b)^2 - 2S_M C_M S_{k\Lambda}(1-\Phi_b)\Phi_b - C_M^2 C_{k\Lambda}\Phi_b^2] \Bigg] \exp\left[-\frac{2kq^2}{4c_0^2} \right] \Bigg\} . \end{aligned} \tag{4}$$

For $c_0^{-1} = c_N^{-1} = C_M^{-1} = 0$, Eq. (2) reduces to the step model,[3–5] while for $c_0^{-1} = \infty$ and $c_N^{-1} = c_M^{-1} = 0$, it reduces to the scattering of two independent blocks of material A and B without any trace of superstructure. This formula can also be used for crystalline-amorphous multilayers by equating f_b to zero.

Using Eq. (2), the high-angle x-ray diffraction pattern of a Nb/Cu multilayer is calculated for a continuous distribution width c_0^{-1} equal to zero, and for different values of the discrete distributions ($c_N^{-1} = c_M^{-1}$) as shown in Fig. 2. In this calculation all correction factors (atomic densities, polarization, absorption, atomic scattering, Lorentz, and Debye-Waller factors) are included. A drastic decrease of the peak intensities and an increase of the linewidth is observed with increasing $c_N^{-1} = c_M^{-1}$. For crystalline-amorphous systems, where this type of disorder was introduced on the amorphous component, the discrete fluctuation only reduces slightly the main peak intensity[12] and wipes out the secondary multilayer fringes.

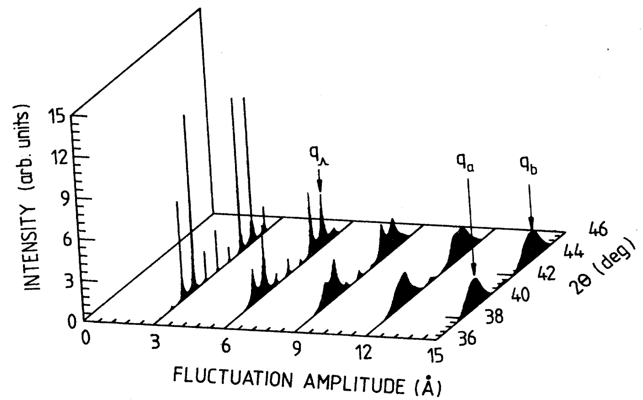

FIG. 2. Evolution of calculated high-angle Nb/Cu spectra for $P=20$, $d_a=2.33$ Å, $d_b=2.08$ Å, $\overline{N}=\overline{M}=24$, $\overline{a}=(d_a+d_b)/2$, as a function of $c_N^{-1}=c_M^{-1}$. For a large fluctuation amplitude only peaks corresponding to q_a and q_b are visible while for smaller amplitudes the q_Λ peaks emerge.

We can intuitively understand our results using a simple argument based on the finite-size fluctuations of a single layer. In this case, layers with different thicknesses contribute to the diffracted intensity. Changing the thickness of layer A will only slightly affect the main peaks around $q_a = 2\pi/d_a$, but can drastically shift the finite-size maxima and minima. These secondary peaks interfere with the main peaks from material B, increase the linewidth and wipe out the superlattice structure.

This is clearly illustrated in Fig. 3 where only discrete variations on the number of atoms of *material A* are taken into account. The peaks of *material B* are drastically affected while the linewidth of the material A peaks stays more or less constant even for relatively large discrete variations. Note that thickness fluctuations in one material tend to broaden diffraction peaks corresponding to the other material.

Previously[6] we showed that a *continuous* distribution on the interfacial distance of the order of the lattice mismatch can explain the observed high-angle line broadening. However, the occurrence of only a few peaks in the low-angle spectra of most crystalline-crystalline multilayers cannot be accounted for using the same continuous distribution. Clearly, a much larger fluctuation (continuous or discrete) is needed to explain this fact. Up to now we showed that a *discrete* distribution on the thickness can also explain the line broadening at high angle, but this distribution has to be of the order of a few times the interatomic distances and might be the candidate to explain the low-angle data.

In Fig. 4 we plot the low-angle diffraction spectra of Nb/Cu multilayers calculated as a function of the discrete distribution ($c_N^{-1} = c_M^{-1}$, $c_0^{-1} = 0$) using the derived kinematical relation. Clearly, a large discrete distribution is necessary to explain the absence of many low-angle peaks. This indicates that it might be possible to obtain a rough estimate for both the discrete and the continuous distributions separately. From the low-angle spectra, the amount of discrete disorder can be estimated.

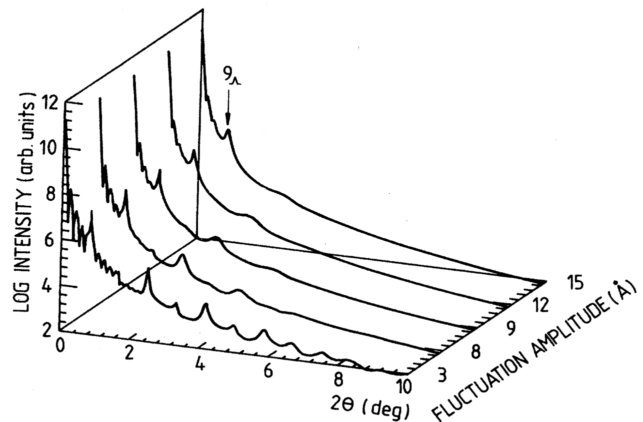

FIG. 4. Evolution of calculated low-angle spectra using the same parameters as in Fig. 2.

This amount can then be fed back into the calculation of the high-angle spectra, with the continuous distribution used only as an adjustable parameter.

Finally, we studied the effect of the lattice mismatch on the line broadening induced by the discrete disorder. Figure 5 shows the high-angle spectra for A and B multilayers with $\Lambda = 100$ Å, $f_a = f_b = 1$, $c_a^{-1} = c_b^{-1} = 6$ Å but for different sets of d values (lattice mismatch). Clearly, for a nearly lattice-matched system the effect of a large discrete distribution is negligible, while in systems with a large mismatch this distribution wipes out all superlattice structure. This proves that the presence of sharp high-angle superlattice diffraction peaks in the nearly matched case is not in contradiction with a substantial amount of discrete roughness.

These results have serious implications on the classical interpretation of x-ray diffraction patterns of superlat-

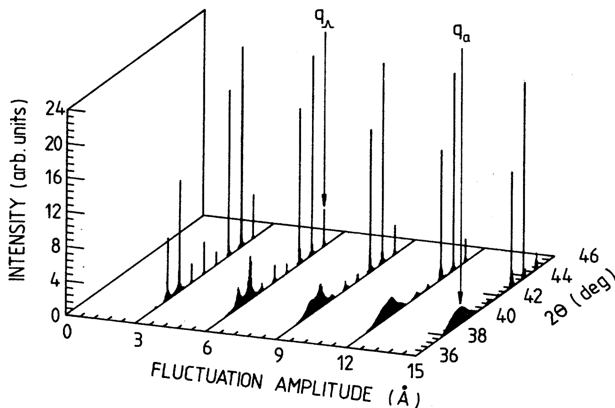

FIG. 3. Evolution of calculated high-angle spectra, using the same parameters as in Fig. 2 except that $c_M^{-1} = 0$. Note that the effect of roughness in one of the superlattice constituents is to broaden the diffraction peaks corresponding to the other.

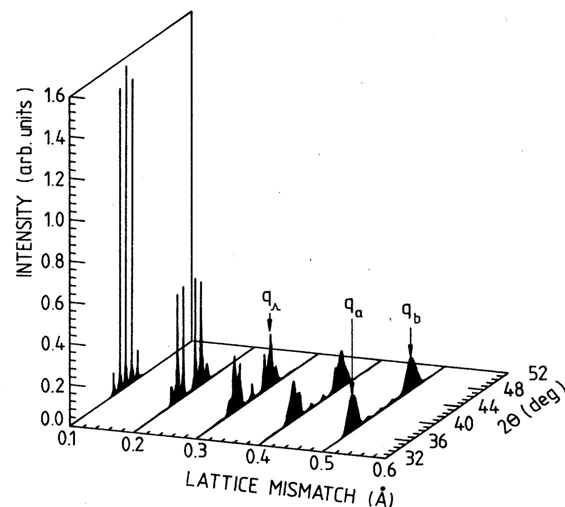

FIG. 5. Evolution of calculated high-angle spectra for $P = 20$, $c_0^{-1} = 0$, $c_a^{-1} = c_b^{-1} = 6$ Å, $\Lambda \simeq 100$ Å for different lattice spacing d values. The results are plotted as a function of the lattice mismatch, $d = d_a - d_b$.

tices. We consider three topics in particular. Lattice-matched semiconductor superlattices grown by molecular-beam epitaxy generally exhibit very narrow high-angle diffraction peaks.[5,16] Considerable caution should be taken when interpreting these data. As shown above, a narrow line width in lattice-matched systems does not necessarily rule out the presence of substantial, discrete, interfacial roughness. Proper intensity calculations are a must. Second, high-angle diffraction spectra have been used to determine the elastic strain in superlattices. The main effect of strain is to change the relative peak intensities of the superlattice satellites.[8,16] However, if the growth conditions (layer-by-layer growth) or the evaporation conditions (fluctuations on the deposition rate) are dissimilar for both materials, the discrete distribution will also give rise to a change in the relative peak intensities.

Finally, the intensities of the low-angle spectra have often been used to reconstruct the composition profile using the Fourier series.[16,17] The ideal composition profile expected for superlattices with no interdiffusion and in the absence of solid solutions is a step function. However, the calculated profile can be largely different and may even have a sinusoidal shape. The interdiffusion length between the layers is then determined from the distance between the maximum and the minimum in the profile. Our results indicate that the absence of higher-order low-angle peaks is not necessarily an indication for interdiffusion, but could be due to roughness.

In summary, we have derived a new diffraction relation for crystalline-crystalline superlattices which includes continuous, as well as discrete, fluctuations. We found that like continuous distributions a discrete distribution can seriously influence the long-range order at high angle in superlattices. Using low-angle diffraction one can independently estimate the amount of discrete fluctuations. These results imply that x-ray linewidths are more sensitive to discrete disorder in lattice-mismatched systems than in lattice-matched systems.

This work was supported by the Belgian Interuniversitair Instituut voor Kern Wetenschappen (IIKW), the Belgian Inter-University Attraction Poles (IUAP) and Concerted Action (GOA) Programme, the U.S. Department of Energy under Contract No. DE-FG03-87ER45332 (at the University of California, San Diego), a North Atlantic Treaty Organization Grant and the Belgian Nationaal Fonds voor Wetenschappelijk Onderzoek (NFWO). Two of us (J.-P.L. and D.N.) would like to thank the Belgian IIKW and NFWO for financial support.

[1]For a recent overview, see *Physics, Fabrication and Application of Multilayered Structures,* edited by P. Dhez and C. Weisbuch (Springer-Verlag, Berlin, in press).

[2]For an overview, see *Synthetic Modulated Structures,* edited by L. L. Chang and B. C. Giessen (Academic, New York, 1985).

[3]I. K. Schuller, Phys. Rev. Lett. **44**, 1597 (1980).

[4]S. Hendricks and E. Teller, J. Chem. Phys. **10**, 147 (1942).

[5]A. Segmüller and A. E. Blakeslee, J. Appl. Crystallogr. **6**, 19 (1973).

[6]J.-P. Locquet, D. Neerinck, L. Stockman, Y. Bruynseraede, and I. K. Schuller, Phys. Rev. B **38**, 3572 (1988).

[7]J.-P. Locquet, D. Neerinck, W. Sevenhans, Y. Bruynseraede, H. Homma, and I. K. Schuller, in *Multilayers: Synthesis, Properties and Non-Electronic Applications,* Materials Research Society Symposia Proceedings, edited by T. W. Barbee, Jr., F. Spaepen, and L. Greer (Materials Research Society, Pittsburgh, 1988), Vol. D 103, p. 211.

[8]D. Neerinck, J.-P. Locquet, L. Stockman, Y. Bruynseraede, and I. K. Schuller, Phys. Scr. **39**, 346 (1989).

[9]S. M. Durbin, J. E. Cunningham, and C. P. Flynn, J. Phys. F **12**, L75 (1982).

[10]P. F. Carcia and A. Suna, J. Appl. Phys. **54**, 2000 (1983).

[11]Y. Fuji, T. Ohnishi, T. Ishihara, Y. Yamada, K. Kawaguchi, N. Nakayama, and T. Shinjo, J. Phys. Soc. Jpn. **55**, 251 (1986).

[12]B. M. Clemens and J. G. Gay, Phys. Rev. B **35**, 9337 (1987).

[13]W. Sevenhans, M. Gijs, Y. Bruynseraede, H. Homma, and I. K. Schuller, Phys. Rev. B **34**, 5955 (1986).

[14]N. Nakayama, K. Takahashi, T. Shinjo, T. Takada, and H. Ichinose, Jpn. J. Appl. Phys. **25**, 552 (1986).

[15]D. Chrzan and P. Dutta, J. Appl. Phys. **59**, 1504 (1986).

[16]A. Segmüller, P. Krishna, and L. Esaki, J. Appl. Crystallogr. **10**, 1 (1977).

[17]R. M. Fleming, D. B. McWhan, A. C. Gossard, W. Wiegmann, and R. A. Logan, J. Appl. Phys. **51**, 357 (1980).